encit 2020

ABCM Associação Brasileira de Engenharia e Ciências Mecânicas

18th Brazilian Congress of Thermal Sciences and Engineering
November 16-20, 2020 (Online)

ENC-2020-0614
A MATHEMATICAL AND NUMERICAL MODEL TO ESTIMATE THE RATE OF CUTTINGS ACCUMULATION IN WELLBORE BOTTOM DURING SHUTDOUWNS OF FLUID CIRCULATION

Pablo Enrique Harbar Penas
Alan Lugarini
Admilson T. Franco
Research Center for Rheology and Non-Newtonian Fluids (CERNN), Universidade Tecnológica Federal do Paraná (UTFPR)
Deputado Heitor Alencar Furtado Street, 5000, 81290-000, Curitiba - PR, Brazil
pablopenas@alunos.utfpr.edu.br, alansouza@utfpr.edu.br, admilson@utfpr.edu.br

Abstract. *During fluid circulation stops in oil and gas wellbore drilling, suspended cuttings will settle towards the bottom. If no action is taken, after some time there is a serious risk of drill pipe sticking. Calculating the particle's settling velocity may be the first step to estimate the cuttings accumulation rate. However, many other factors have to be accountable for, such as drilling fluid rheology, geological properties, and operational conditions before the circulation stop. A systematic approach for estimating the cutting accumulation rate is still lacking in specialized literature. This work presents a simple numerical procedure to calculate the time evolution of the cuttings bed height. The fluids considered are viscoplastic and thixotropic. A series of case studies are provided to assess the model behavior for steady-state and transient cuttings settling. It is expected that this model can assist field engineers in decision-making processes.*

Keywords: *Cuttings transport, stop circulation, particle settling, thixotropy*

1. INTRODUCTION

Understanding the settling phenomenon in thixotropic non-Newtonian fluids is crucial to assess cuttings transport and accumulation in wellbores. During drilling operations, the cuttings removed from the wellbore bottom are carried upwards by the drilling fluid, which has many non-Newtonian characteristics. The fluid circulation might stop due to a variety of reasons, for instance, lack of pumping power or missing fluid. This can lead to the accumulation of cutting in the bottom, threatening the drill string motion. Great undesirable costs will have to be expended in the case of pipe sticking (Muqeem et al., 2012).

Cuttings transport in vertical wellbores has been widely studied since the early studies of Piggot (1941). Most of them are investigations on operational criteria for efficient hole cleaning, such as the mechanistic model of (Clark & Bickham, 1994). The case of stop circulation, on the other hand, can be approached as a particle settling phenomenon, since the drilling fluid is almost entirely stationary. As a means to estimate the cuttings bed growth by settling, Mitchell and Miska (2011), approximate the slip velocity by the theoretical terminal velocity, and based on the displacement of a single particle settling at terminal velocity, they predicted the bed height after thirty minutes. This leads to a reasonable approximation of the cuttings accumulation rate. However, mass conservation was not respected. Fluid flow through the boundary set between the suspension and the packed bed was neglected. Also, the slip velocity would be better approximated by the terminal velocity corrected by a hindered settling factor.

There are many procedures to determine the particle slip velocity. In steady-state regime, the forces acting on the particle (stationary drag and net gravity) balance out, leading to a null acceleration. Thus, the slip velocity can be calculated provided that the drag coefficient (Cd) is known. Cd can be obtained through Cd-Re charts, or drag correlations (Concha, 2014). An alternative method consists in introducing a relationship between the terminal Reynolds number (Re) and the Archimedes number (Ar) (Kelessidis, 2004), leading to an explicit equation to determine the slip velocity. Although it sounds more convenient to use explicit functions, this method is less accurate since the Re-Ar fitting introduces additional errors.

Particles settling in a thixotropic fluid experience a different motion. These particles might also reach steady-state, but it will take considerably longer. The most common numerical approach to transient motion in thixotropic fluids is to treat the fluid as a continuous phase and apply Eulerian tracking to the solids. Walters (1992) presented a numerical model to simulate particle settling in transient motion and compared with experimental data, achieving good qualitative results. This approach requires a great number of computational resources for simulating so many particles, seeing that for each particle, velocity and position must be updated every timestep.

Motivated by the lack of a comprehensive model for cuttings accumulation rate in wellbore bottom, the present work is set to seek such goal. In the following text, an estimate method for the transient bed height caused by stop circulation of thixo-viscoplastic fluid is developed. It is expected that this model will aid drilling engineers in decision-making processes. The model assessment is divided into two parts. First, non-thixotropic drilling fluids are simulated and the accumulation rate is calculated. Then, thixotropy is considered and the bed height evolution is analyzed.

2. MATHEMATICAL MODEL

Initially, drilling fluid is pumped through the drill string and it returns through the annular space defined between the string outer diameter (D_i) and the well diameter (D_e), as illustrated in Figure 1.a. In the returning path, the drilling fluid carries away the cuttings created in the perforation. In the event of a stop circulation, the cuttings that were ascending will settle towards the bottom forming the packed bed. Gelification is the desired effect that can retard the settling rate of these particles. It is recommended that field engineers use thixotropic fluids which have a time-depend behavior, namely the viscosity increase over time, which as a result reduces the cuttings settling velocity.

To fully understand the mechanisms of the packed bed height evolution it is proposed to perform a control volume analysis around the packed bed. Figure 1.b shows the boundaries of the annular transient control volume, limited by the interface between suspension and packed cuttings with solids volume concentration ϕ_0 and $\phi_{\max}$ respectively.

The main challenge is to determine the suspension solids volume fraction. According to the theory of *Batch Sedimentation* (Rao et al., 2002), an initially well-mixed suspension will separate into three different phases: a clear zone of fluid at the top, followed by a well-mixed suspension at the average concentration and the sediment lying at the bottom. Batch Sedimentation effects, as solids concentration distribution, can be neglected if the domain is sufficiently larger than the region of interest. Thus, the hypothesis of constant volume fraction of the suspension is assumed.

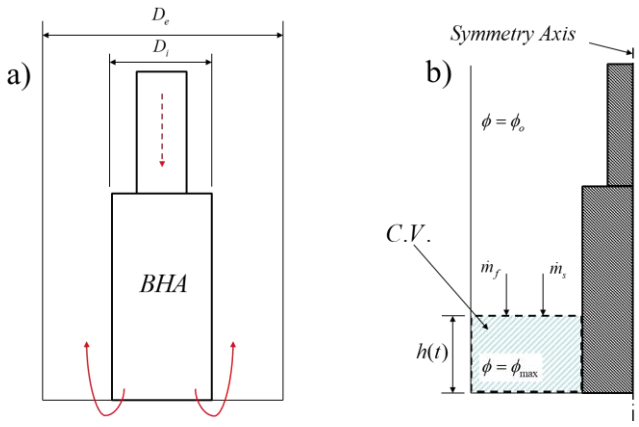

Figure 1. a) Simplified sketch of a bottom hole assembly (BHA) during drilling operations, where red arrows indicate mudflow. b) Control volume analysis.

Solids mass flux inwards is assumed to be globally unidirectional and consists of the relative settling effect regarding the packed bed boundary motion. Fluid flow is a result of the rising boundary movement since the fluid is at rest when the circulation has been stopped. With these assumptions, an integral mass balance in the control volume illustrated in Fig. 1.b yields

$$\dot{h} = \frac{\bar{V}_t}{\left(\frac{\phi_{bed}}{\phi_{susp}} - 1\right)\left(1 - \frac{\rho_f}{\rho_s}\right)} \tag{1}$$

Where $\bar{V}_t$ is the average terminal velocity, A_T is the annular area, ϕ_{susp} is the solids volume fraction of the suspension and ϕ_{bed} is the maximum solids concentration of the packed bed. The average terminal velocity can be approximated by the terminal velocity of a single particle corrected by a hindered settling factor, which accounts for the effects of the neighboring particles. Therefore, the control parameters are density ratio ρ_f / ρ_s, concentration ratio ϕ_{bed} / ϕ_{susp}, and the average terminal velocity.

As described in the literature (White & Walton, 1937), there are five fundamentals sphere packing modes, and each has a respective void volume fraction. In this work, the single stagger mode is assumed to best represent the packed bed, with a respective solids volume fraction of 0.6. The suspension solids volume fraction depends on the drilling parameters

before stop circulation. The mass flow of solids extracted from the wellbore is a product of the rate of penetration (ROP) and the drilled area A_p. The solids concentration of the suspension is the ratio between the area occupied by the particles and the annular area, evaluated in an imaginary layer, shown in Figure 2, that moves at the same velocity as the mixture. The concentration is defined as:

$$\phi_{susp} = \frac{A_s}{A_T} = \frac{A_s \bar{V}_p}{A_T \bar{V}_p} = \frac{Q_s}{A_T \bar{V}_p} \tag{2}$$

And the mixture velocity is defined as:

$$V_{mix} = \frac{Q_s + Q_f}{A_T} \tag{3}$$

The definition of slip velocity is the difference between the particle absolute velocity $\bar{V}_p$ and the continuous phase velocity V_f before stop circulation and can be resumed as the relative velocity between phases. It is convenient to approximate the fluid velocity as the mixture velocity; however, this assumption is only reasonable for dilute flows. Equation (4) describes the slip velocity regarding the approximation $V_f \approx V_{mix}$.

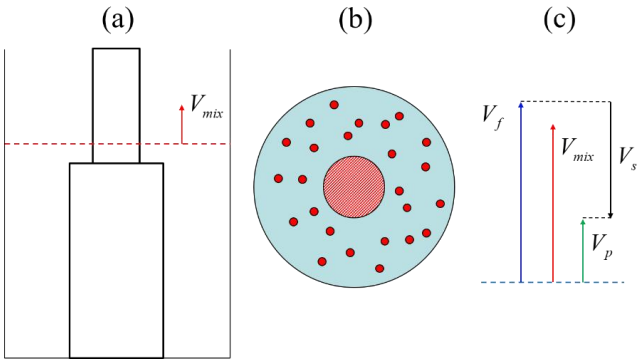

Figure 2. a) Imaginary layer moving at mixture velocity, b) illustration of the solids distribution, c) velocity vectors.

$$\bar{V}_s = \bar{V}_p - V_{mix} \tag{4}$$

Equation (2) can be rewritten combined with eq. (4) as:

$$\phi_{susp} = \frac{Q_s}{A_T \left(V_{mix} + \bar{V}_s \right)} \tag{5}$$

Seeing that sedimentation occurs after the circulation stops, one can describe accurately the slip velocity as the terminal velocity of a particle settling in a fluid at rest. Therefore, it is convenient to modify eq. (5) with the terminal velocity:

$$\phi_{susp} = \frac{Q_s}{A_T \left(V_{mix} - \left| \bar{V}_s \right| \right)} = \frac{Q_s}{A_T \left(V_{mix} - \bar{V}_t \right)} \tag{6}$$

Combining Eqs. (3) and (6) yields the correlation that estimates the suspension solids volume concentration based on drilling operation parameters:

$$\phi_{susp} = \frac{Q_s}{Q_s + Q_f - A_T \bar{V}_t} = \frac{A_p \left(ROP \right)}{A_p \left(ROP \right) + Q_f - A_T \bar{V}_t} \tag{7}$$

Equation (7) highlights the relationship between the annular space and the solids concentration. Usually, when a stop is required in drilling operations, the drilling column is retracted approximately 27 meters upwards, dislocating both fluid and cuttings. That is why there is no reason to differentiate volume fraction on the BHA (bottom hole assembly) and the

region right above it, despite the change in inner diameters, and can be surely be approximated by the volume fraction of the smallest diameter region, that would be a critical case regarding the cuttings accumulation rate. At last, the flow characteristics must verify minimum cleaning conditions, meaning that the fluid must be able to transport the cuttings. This verification must minimally satisfy the inequality:

$$V_{mix} > \bar{V}_s \tag{8}$$

Currently, the mathematical model supports both permanent and transient regimes, depending on whether the thixotropy effect is being accounted. As to the first, cuttings initiate movement at terminal velocity since the corresponding time for the particle to achieve terminal velocity from rest is negligible if compared to the critical time that sedimentation takes to compromise the wellbore stability.

Neighboring particle effects are accounted for through hindered settling functions (Richardson & Zaki, 1997), which determines the level of hindering exerted by a population of particles, leading to an averaged global settling rate $\bar{V}_t$ applied to the discrete phase.

$$\bar{V}_t = V_t f(\phi) \tag{9}$$

For Newtonian fluids, hindered settling function $f(\phi)$ has been widely studied and can be found in a form of $f(\phi) = (1-\phi)^{n_h}$, where n_h is the power index and varies according to the terminal Reynolds number. Table 1 shows correlations for the power index based on Re, obtained empirically for Newtonian fluids.

Table 1. Correlations for hindered settling function power index for Newtonian fluids.

Range of Re_t	**Index** n_h
$\mathrm{Re} < 0.2$	4.65
$0.2 < \mathrm{Re} < 1$	$4.35\,\mathrm{Re}^{-0.03}$
$1 < \mathrm{Re} < 500$	$4.45\,\mathrm{Re}^{-0.10}$
$\mathrm{Re} > 500$	2.39

Settling in shear-thinning fluids present a unique behavior, as sedimentation progresses there is a tendency for agglomeration of particles (Moreira et al., 2017), due to the decrease of apparent viscosity for higher shear rates. Thus, Newtonian forms of the hindered settling functions can only be used for estimating the hindered settling velocity for power-law indexes close to the Newtonian limit.

Solution for transient state involves Newton's second law discretization. Based on weight, drag, buoyancy and virtual mass forces, yields the expression for the motion of a single particle:

$$m\frac{dV}{dt} = (W - B) - F_{vm} - F_D = mg(\rho_s - \rho_f) - \frac{m}{2}\frac{dV}{dt} - \frac{1}{2}\rho_f V^2 S_m C_D(V,t) \tag{10}$$

Solving for $\frac{dV}{dt}$:

$$\frac{dV}{dt} = \frac{2}{3}\left(\frac{(\rho_s - \rho_f)g}{\rho_f} - \frac{3\rho_f}{4 d_s \rho_s} V^2 C_D(V,t)\right) \tag{11}$$

Seeing that the method to determine the drag coefficient is implicit, Eq. (11) cannot be solved analytically. Therefore, it must be solved numerically. The expression for single particle acceleration is an initial value problem, since it starts from rest at $t = 0$, and can be written as $y' = F(t,y)$, with $y(t_0) = 0$.

2.1 NON-NEWTONIAN DRAG

Drilling fluids have a viscoplastic behavior. The yield stress helps retain small cuttings from settling. In the present work, the viscoplastic nature of the drilling fluid is represented by the Herschel-Bulkley (HB) model:

$$\tau = \tau_y + K\dot{\gamma}^n \tag{12}$$

where τ_y is the yield stress, K is the consistency factor, $\dot{\gamma}$ is the shear rate and n is the power index. The drilling fluid's observed gelification is treated by a thixotropic model. In this work, it is considered that thixotropy changes the magnitude of the yield stress, with a duration equivalent to gelification time t_q (Chang et al., 1999), and described by two parameters: gel stress τ_g and dynamic yield stress τ_0.

$$\tau_y(t) = \frac{\tau_g - \tau_0}{1 + t/t_q} + \tau_0 \tag{13}$$

Due to yield stress, it is convenient to introduce a new non-dimensional group that relatively accounts for the magnitude of gravitational and stress-induced forces (Chhabra & Group, 2007), the yield coefficient. This coefficient is measured in conditions where $\bar{V}_p = 0$.

$$Y_G = \frac{\tau_y}{g d_s (\rho_s - \rho_f)} \tag{14}$$

The drag coefficient method used on this work is based on a numerical study of a flow over a sphere (Gavrilov et al., 2017). Schiller-Nauman drag correlation for Newtonian fluids was adapted applying a correction function Y_{HB}:

$$C_D = \frac{24}{\mathrm{Re}} Y_{HB}(Q, Bn, n) \tag{15}$$

The correction function Y_{HB} can be described as the combination of plastic effects Bn and the correction function for power-law fluids:

$$Y_{HB}(\mathrm{Re}, Bn, n) = Y_{PL}\left(Q(\mathrm{Re}, Bn), n\right) + C_{HB1}(n) Bn + C_{HB2} Bn^{\frac{n}{n+1}} \tag{16}$$

$$Y_{PL}(\mathrm{Re}, n) = 1 + C_{PL1}\tilde{n} + C_{PL2}\tilde{n}^2 + \left(0.15 + C_{PL3}\tilde{n} + C_{PL4}\tilde{n}^2\right)\mathrm{Re}^{0.687 + C_{PL5}\tilde{n} + C_{PL6}\tilde{n}^2} \tag{17}$$

The reverse power index $\tilde{n} = 1 - n$ was used to simplify the equations. Results were validated for ranges of $0 \le \mathrm{Re} \le 200$, $0 \le Bn \le 100$ and $0.3 \le n \le 1$.

An expression for slip velocity comes from Newton's second law, based on drag, weight, and buoyancy, as:

$$V_s = \sqrt{\frac{2}{C_D \rho_f}\left[\frac{2}{3}(\rho_s - \rho_f) d_s g\right]} \tag{18}$$

The solution for the terminal velocity includes numerical iterations employing eq. (18) and drag coefficient equations.

3. NUMERICAL MODEL

The fourth-order Range-Kutta discretization (RK4) was employed to solve Eq. (22) explicitly for single particle motion. The discretized system of equation form RK4 is as it follows:

$$y_{n+1} = y_n + \frac{h}{6}(k_1 + 2k_2 + 2k_3 + k_4) \tag{19}$$

$$\begin{aligned} k_1 &= F(t_n, y_n) \\ k_2 &= F\left(t_n + \frac{h}{2}, y_n + \frac{h}{2}k_1\right) \\ k_3 &= F\left(t_n + \frac{h}{2}, y_n + \frac{h}{2}k_2\right) \\ k_4 &= F(t_n + h, y_n + hk_3) \end{aligned} \tag{20}$$

$$t_{n+1} = t_n + h \tag{21}$$

Where h is the timestep, k_1 is the slope at the beginning of the interval, k_2 is the slope at the midpoint of the interval, k_3 is also the slope at the midpoint but using k_2 and k_4 is the slope at the end of the interval. Applying RK4 method leads to convergence for larger timesteps than Euler's method, for instance, because the next value is calculated based on an estimated average slope through ponderation of the slopes k_i.

Solving for particle velocity yields:

$$V_{n+1} = V_n + \frac{h}{6}\left(k_1 + 2k_2 + 2k_3 + k_4\right) \tag{22}$$

$$F\left(t_n, V_n\right) = \frac{\left(\rho_s - \rho_f\right)g}{\rho_f} - \frac{3\rho_f}{4d_s\rho_s} V_n^2 C_D\left(V_n, t_n\right) \tag{23}$$

Hindered settling effects were adapted for transient regimes by replacing the terminal Reynolds number by the instantaneous Reynolds number in Eqs. (24) and (25) when evaluating the power index n_h. The level of hindrance must only be applied to the velocity increase at t_{n+1}, otherwise, there would be an overlapping of the hindered settling effects from previous temporal states.

$$f\left(\phi, \mathrm{Re}\right) = \left(1-\phi\right)^{n_h} \tag{24}$$

$$\bar{V}_{n+1} = \bar{V}_n + \frac{h}{6}\left(k_1 + 2k_2 + 2k_3 + k_4\right) f\left(\phi, \mathrm{Re}_{n+1}\right) \tag{25}$$

There is an implicit calculation scheme to solve Eq. (25), Re_{n+1} must be calculated based on $\bar{V}_{n+1}$ so that the first is correctly assigned. This calculation scheme is initialized solving Re_{n+1} with V_{n+1} and after each iteration, $\bar{V}_{n+1}$ is updated until it reaches the convergence criteria. Hence Eqs. (22) and (25) must be solved simultaneously. Finally, the expression for the accumulation rate for transient states is:

$$\dot{h}_{n+1} = \frac{\bar{V}_{n+1}}{\left(\dfrac{\phi_{leito}}{\phi_{susp}} - 1\right)\left(1 - \dfrac{\rho_f}{\rho_s}\right)} \tag{26}$$

Given that the cuttings begin to settle from rest, the initial value for the accumulation rate is $\dot{h}_0 = 0$. Figure 3 illustrates the numerical scheme that solves steady and transient flows. It was possible to simulate 18000 seconds of sedimentation in 255 seconds of computational time in the Google Colab Research Python application. Relevant industrial simulations would only require a fraction of that physical time, meaning results could be obtained in nearly real-time.

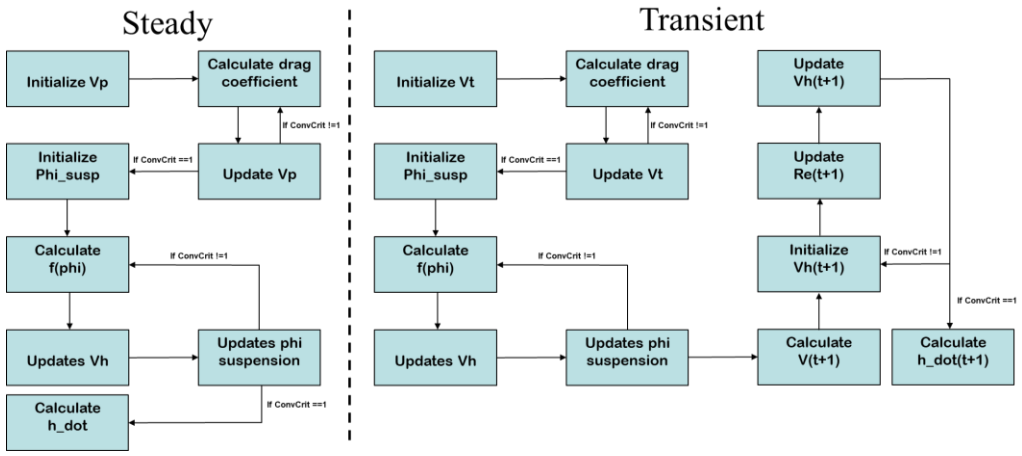

Figure 3. Flowchart of the numerical scheme.

4. STEADY-STATE RESULTS

This section is focused on reporting results for non-thixotropic fluids. Table 2 contains geometric and operational data for drilling parameters and Table 3 shows the rheological properties of fictitious drilling fluids. Besides that the viscoplastic fluids of Table 4, results for Newtonian fluids are presented for comparison: water ($\rho_f = 998.15$ kg/m³, $\mu = 1$ mPa.s^{-1}) and diesel oil ($\rho_f = 836.39$ kg/m³, $\mu = 2.55$ mPa.s^{-1}).

Table 2. Geometrical and operational drilling parameters.

Description	Outer diameter	Inner diameter	Flow rate			Rate of penetration	Cuttings density			Bed solids concentration
Symbol	D_e	D_i	Q_f			ROP	ρ_s			ϕ_{bed}
Value	8.5”	6.75”	200 gpm	350 gpm	500 gpm	12 m/h	2983.7 kg/m³ (Basalt)	2696.1 kg/m³ (Shale)	2324.6 kg/m³ (Halite)	0.6045

Table 3. Rheological properties of fictitious non-thixotropic fluids.

	Fluid 1	Fluid 2	Fluid 3
K	0.03	0.03	0.03
n	1	0.85	0.85
τ_y	1 Pa	1 Pa	4 Pa
ρ_f	1198.3 kg/m³	1198.3 kg/m³	1198.3 kg/m³

The yield coefficient was calculated based on the observation of motion/no motion of the particles under gravity. Through Figure 4 and Figure 5, the yield coefficient is obtained for the largest diameter that corresponds to a null accumulation rate.

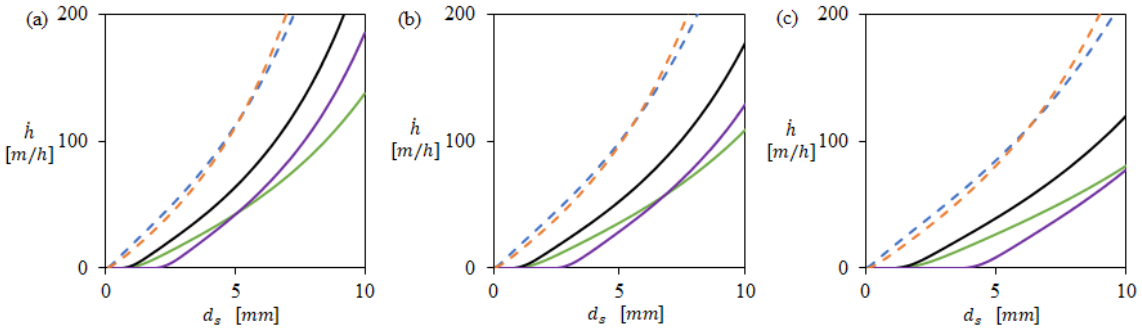

Figure 4. Comparison for accumulation rate at 200 gpm for: (a) Basalt, (b) Shale, (c) Halite. Blue dashed line represents water, dashed orange line is diesel oil, the green line is fluid 1, the black line is fluid 2 and the purple line is fluid 3.

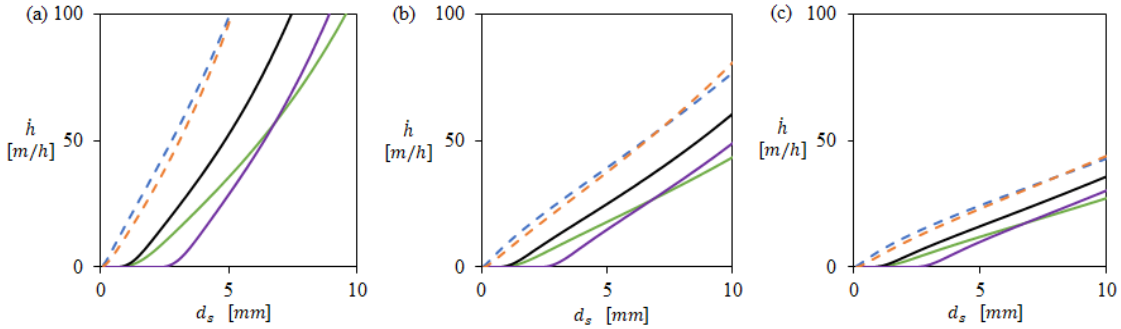

Figure 5. Comparison for accumulation rate for shale geology at: (a) 200 gpm, (b) 350 gpm, (c) 500 gpm. Blue dashed line represents water, dashed orange line is diesel oil, the green line is fluid 1, the black line is fluid 2 and the purple line is fluid 3.

Figure 4 indicates that geology can affect the critical diameter, for which particles are unable to settle. Higher cuttings densities result in higher accumulation rates as well as enabling smaller particles to settle. Higher flow rates can efficiently diminish the accumulation rate, seeing that it results in more dilute suspensions before stopping circulation. The yield coefficient reported varies in range from 0,103 to 0.132, depending on the density ratio. Results come with good agreement with values reported by Attapatu et. al (1986), who experimentally obtained values in the range of 0.095-0.111 for the yield coefficient based on the same observations for yield stress.

5. TRANSIENT RESULTS

Analysis of thixotropic drilling fluids is included in this section. Operating characteristics are the same as steady-state, Table 2. However, this case study is limited to a flow rate of 200 gpm and shale type geology. Fictitious fluids are described in Table 4 and parameter variation was exclusive to gelification time and gel stress. The critical yield stress τ_y was used as a reference value for a temporal grid performance test. It was found that a timestep of 0.001 s was suitable for application seeing as the critical yield stress value of 2.41 Pa had approximately 1% of deviation from the value of 2.44 Pa obtained for a timestep of 0.0001 s. Fluids 4 and 5 have higher yield stress and they were able to enclosure 2.5 mm particles before thixotropic structuring had finished. The yield coefficient for both cases was found to be 0.127.

Table 4. Fictitious thixotropic fluid characterization.

	Fluid 1	Fluid 2	Fluid 3	Fluid 4	Fluid 5
K	0.03	0.03	0.03	0.03	0.03
n	0.85	0.85	0.85	0.85	0.85
τ_0	1 Pa	1 Pa	1 Pa	1 Pa	1 Pa
τ_g	4 Pa	4 Pa	4 Pa	8 Pa	8 Pa
ρ_f	1198.3 kg/m³	1198.3 kg/m³	1198.3 kg/m³	1198.3 kg/m³	1198.3 kg/m³
t_q	180 s	1800 s	18000 s	1800 s	18000 s

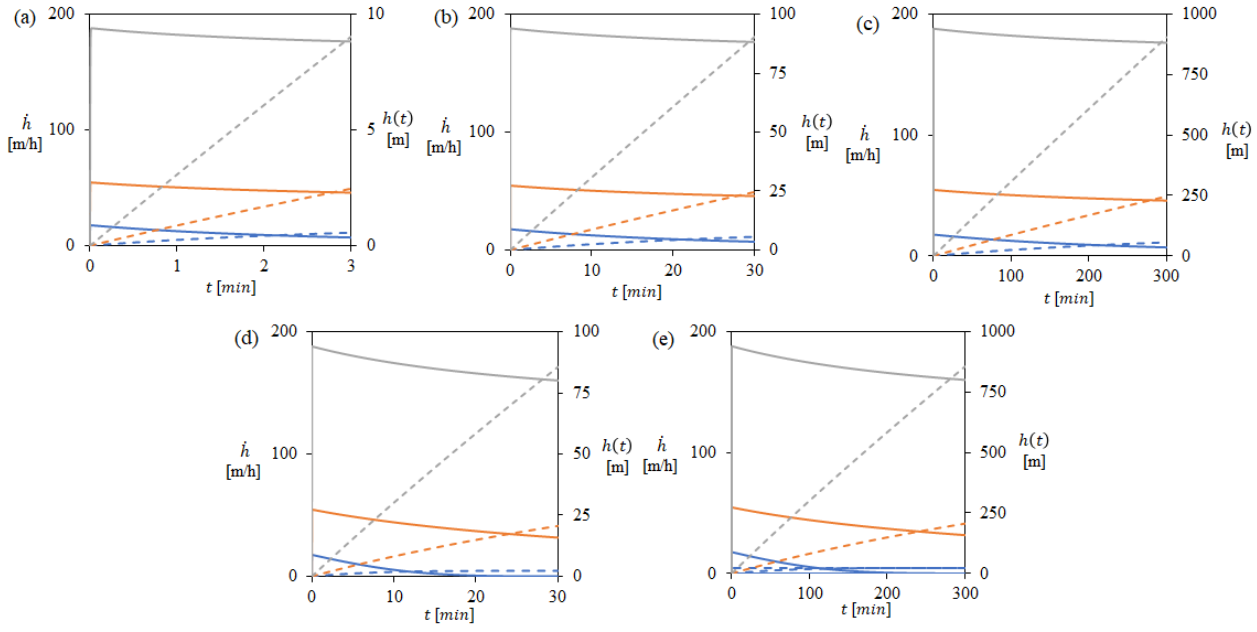

Figure 6. Results for accumulation rate for: (a) Fluid 1, (b) Fluid 2, (c) Fluid 3, (d) Fluid 4, (e) Fluid 5. The dashed line represents bed height h(t) and the solid line represents the accumulation rate $\dot{h}$. In blue denotes 2.5 mm particles, in orange 5 mm and gray denotes 10 mm particles.

Figure 6 suggests that higher gel stresses can delay bed formation by reducing the accumulation rate. Besides, gelification time dictates the time delay for gel stress effects and smaller particles encasement. High yield stress is not necessary during pumping in drilling operations, because of increased friction. Thus, the gelification property must be enhanced, as a combination of higher gel stress and shorter gelification time. The corresponded time that takes for the

cuttings to reach terminal velocity is insignificant compared with gelification time. So as to encase 10 mm particles, high gel stress might not be sufficient, and a denser fluid should be projected, that would require a smaller force due to shear stress to balance out the net weight.

6. CONCLUSIONS

This paper presented an estimate model for cuttings accumulation rate on vertical wellbores for thixo-viscoplastic drilling fluids. Results for steady-state agreed with the range of yield coefficient values reported in the literature. Reported data have a physical meaning that can be used for helping field engineers evaluate risks in cases of circulation stops. In the case of pipe sticking, the fluid flow rate could be enhanced moments before circulation has stopped to reduce the accumulation rate as suggested by steady-state results. Typical times associated with pipe sticking can be delayed by thixotropic gel stress avoiding potential accumulation risks.

It is expected from this model to be easily reproduced. Improvements such as new correlations for drag coefficient and the development of new forms of hindered settling function for non-Newtonian fluids will hereafter be implemented.

REFERENCES

Atapattu, D. D., Chhabra, R. P., Tiu, C., & Uhlherr, P. H. T. (1986). The effect of cylindrical boundaries for spheres falling in fluids having a yield stress. In *9th Australasian Fluid Mechanics Conference, Auckland*.

Chang, C., Nguyen, Q. D., & Rønningsen, H. P. (1999). Isothermal start-up of pipeline transporting waxy crude oil. *Journal of Non-Newtonian Fluid Mechanics*, *87*(2–3), 127–154. https://doi.org/10.1016/S0377-0257(99)00059-2

Chhabra, R. P., & Group, F. (2007). Bubbles and Droplets. In *Technology*.

Clark, R. K., & Bickham, K. L. (1994). Mechanistic model for cuttings transport. *Proceedings - SPE Annual Technical Conference and Exhibition*, *Delta*, 139–153.

Concha, F. (2014). *Fluid Mechanics and Its Applications Solid–Liquid Separation in the Mining Industry*.

Gavrilov, A. A., Finnikov, K. A., & Podryabinkin, E. V. (2017). Modeling of steady Herschel–Bulkley fluid flow over a sphere. *Journal of Engineering Thermophysics*, *26*(2), 197–215. https://doi.org/10.1134/S1810232817020060

Mitchell, R. F., & Miska, S. Z. (2011). Fundamentals of Drilling Engineering. SPE Textbook Series. Vol. 12. Society of Petroleum Engineers, Richardson, Texas.

Kelessidis, V. G. (2004). An explicit equation for the terminal velocity of solid spheres falling in pseudoplastic liquids. *Chemical Engineering Science*, *59*(21), 4437–4447. https://doi.org/10.1016/j.ces.2004.07.008

Moreira, B. A., de Oliveira Arouca, F., & Damasceno, J. J. R. (2017). Analysis of suspension sedimentation in fluids with rheological shear-thinning properties and thixotropic effects. *Powder Technology*, *308*, 290–297. https://doi.org/10.1016/j.powtec.2016.12.034

Muqeem, M. A., Weekse, A. E., & Al-Hajji, A. A. (2012). Stuck pipe best practices - A challenging approach to reducing stuck pipe costs. *Society of Petroleum Engineers - SPE Saudi Arabia Section Technical Symposium and Exhibition 2012*, 756–765.

Pigott, R. J. S. (1941, January 1). Mud Flow In Drilling. American Petroleum Institute.

Rao, R., Mondy, L., Sun, A., & Altobelli, S. (2002). *Rao_et_al-2002-International_Journal_for_Numerical_Methods_in_Fluids*. *483*(May 2001), 465–483. https://doi.org/10.1002/fld.246

Richardson, J. F., & Zaki, W. N. (1997). Sedimentation and fluidization: Part I. *Process Safety and Environmental Protection: Transactions of the Institution of Chemical Engineers, Part B*, *75*(Suppl), S82–S100. https://doi.org/10.1016/s0263-8762(97)80006-8

Walters, K., & Tanner, R. I. (1992). The motion of a sphere through an elastic fluid. *Transport Processes in Bubbles, Drops, and Particles, Hemisphere, New York, NY*, *1*, 992.

White, H. E., & Walton, S. F. (1937). Particle Packing and Particle Shape. *Journal of the American Ceramic Society*, *20*(1–12), 155–166. https://doi.org/10.1111/j.1151-2916.1937.tb19882.x